SLAC-PUB-95-6970
August 1995

INITIAL STUDIES OF ELECTROMAGNETIC SHOWER ENERGY DEPOSITION IN SMALL-BORE SUPERCONDUCTING UNDULATOR STRUCTURES IN LINAC ENVIRONMENTS*

T. Cremer, W. R. Nelson, and R. Tatchyn
Stanford Synchrotron Radiation Laboratory, Stanford Linear Accelerator Center,
Stanford University, Stanford, CA 94309, USA

Abstract

One of the more promising technologies for developing minimal-length insertion devices for linac-driven, single-pass Free Electron Lasers (FELs) operating in the x-ray range is based on the use of superconducting (SC) materials. Despite its advantage of minimal length, however, SC technology can present difficulties for insertion device design and operation. One critical problem, as observed, e.g., by Madey and co-workers in their initial (25 MeV) FEL experiments, was the frequent quenching induced by scattered electrons upstream of their (bifilar helical) SC device. In view of the short-term stability required of undulators for user facilities, we have initiated a systematic investigation of these earlier results to determine whether quenching could become similarly probable in SLAC's (10-15 GeV) Linac Coherent Light Source (LCLS), a 1.5 Å FEL. Postulating that the onset and spread of normal zones are precipitated by directly-scattered or bremsstrahlung-propagated particle energy deposited into the SC material or into material contiguous with it, we have used the EGS4 particle-tracking code developed at SLAC to perform studies of scattered-particle energy deposition into SC structures with geometries comparable to a small-bore bifilar helical undulator. Preliminary numerical results for both the Madey and SLAC LCLS cases have been obtained.

*Work supported in part by the Department of Energy Offices of Basic Energy Sciences and High Energy and Nuclear Physics, and Department of Energy Contract DE-AC076SF0015.

(Presented at the 17th International Free Electron Laser Conference (FEL95) and 2nd Annual FEL Users' Workshop, New York, New York, August 21-25, 1995)

1. Introduction

The 1.5 Å LCLS, an FEL designed for 10-15 GeV operation in the Self Amplified Spontaneous Emission (SASE) mode on the last 1-km section of the 3-km linac at SLAC [1], is currently being assessed with respect to superconducting (SC) vs. alternative technologies (e.g., hybrid/permanent magnet (PM)) for the development of its long insertion device [2]. In recent simulations, e.g., a bifilar helical SC device (see Fig. 1a) with λ_u=2 cm, 6 mm inner diameter, and a 1.8 T field was found to require a 30 m length for saturating at 1.5Å on a 15 GeV linac - ~40% shorter than an alternative hybrid/PM design [3]. Despite this fundamental advantage, however, it is known that SC technology is highly non-trivial and can present challenging problems in design and operation.

One such problem, first observed in a similar SC device by Madey and co-workers at Stanford [4], was quenching precipitated by a thin beam-monitoring Mo foil placed just upstream of their device [5]. The conventional hypothesis is that the quenching was induced by temperature rise following the accumulation of scattered-particle and electromagnetic (EM) shower energy within the SC volume [6]. Analogously to the Madey experiment - although for the purpose of energy-tail scraping [7] as opposed to beam monitoring - an upstream collimator with a small (40 - 100μ diameter) aperture may also need to be placed in proximity to the LCLS device. This, of course, raises the possibility that conditions for quenching at SLAC may, to a greater or lesser extent, also be met. Since a longer-term goal of the LCLS research and development (r&d) program is to provide technology for a coherent x-ray user facility - which entails stringent short-term stability for its undulator -, the LCLS research group has initiated a computational and experimental study of quenching in the insertion device proposed for SLAC. In this paper, initial results in the computational part of this program, obtained with the EGS4 particle-tracking code [8] developed by one of us (WRN) at SLAC, are presented.

2. The EGS4 code

EGS4 is a general-purpose software package for the Monte Carlo simulation of the coupled transport of electrons and photons in an arbitrary environment configured or bounded by an arbitrary geometry [9]. Due to its comprehensive data base of scattering cross sections, it can accurately simulate interactions spanning the 10 KeV - 1 TeV+

energy range. In a common mode of study, the geometry of the system of interest is defined and divided up into volumetric regions; the location, attitude, and energy of a selected particle entering the region are defined; and the energy deposited into the defined volumes is calculated as the particle and its scattered offspring propagate through and out of the system. Since the occurrence, channels, and cross section of each scattering event are statistically chosen, a sufficient number of initial particles must be modeled through the system to obtain adequate statistics [10]. The average energy absorbed in any volume of interest can then be expressed as a fraction of the initial particle's total energy. In a typical problem, the boundaries of the volumetric regions may coincide with the different materials and fields constituting those regions, and more detailed energy-deposition profiles in any volume of interest are obtained by subdivision to the required resolution. Although EGS4 is capable of simulating any practical configuration, for many systems adequate estimates of deposited energy density can be obtained from simplified or symmetrized versions of their geometries. This approach has in fact been utilized in the present study (see Fig. 1). This allows the scattering simulations to be started in a single (longitudinally axis-centered) plane, and the results to be averaged analytically about the forward axis, which significantly reduces the time required for a statistically robust multi-parameter case study. Justification for the symmetrization is based in part on the high directionality of particle cascades at ultrarelativistic energies and on the equivalent depth of the undulator presented to an individual cascade. A further simplifying assumption in the present study has been to omit the undulator's magnetic field. This is partly justified for the LCLS by the high average energy of the initial and scattered particles (most of which will be deflected only very slightly by the (1T-3T) undulator fields). In the Madey case the field omission is less justifiable (the ~ 9 cm turning radius of a 25 MeV electron in a 1 T field is only 3 times larger than the undulator period), since more than half of the lower-energy electrons are strongly deflected by the SC fields. In this regard, the results of our simulations of Madey's experiment should not be considered valid to better than an order of magnitude.

3. Physical and dimensional parameters of the Madey and LCLS devices

The Madey experiment utilized a potted undulator structure [4]. First, the bifilar SC coil was wound onto a pre-machined helical Delrin mandrel with a pre-drilled bore. For in-vacuum operation, a cylindrical Cu duct was installed in the bore. Following the first winding, an Al separator was placed over the bifilar coil and a second, solenoidal coil was wound over it along the length of the undulator. Following the second winding, the assemblage was slipped into a larger-diameter Al tube and the space between the tube and the undulator was vacuum-impregnated with epoxy. A cross section of this structure is depicted in Fig. 2. For the experiment, the whole structure was placed inside a liquid-He cryostat and connected to the linac vacuum through flanged terminations. A schematic side view of this geometry, including a representation of the scattering foil that precipitated the quenching, is shown in Fig. 3. Since the LCLS undulator will also be located in a cryostat, and since its energy-tail collimator will also be located upstream, the layout in Fig. 3 can be used to represent both the Madey and LCLS undulators for the EGS4 studies. The dimensions and materials distributions associated with each of the two cases are tabulated in Fig. 3. In particular, we can calculate that the volume of the annular SC rings, viz., $(\pi/4)$(SC_axial_thick)(SC_OR^2 - SC_IR^2), is approximately 3.8 cm^3 for the Madey case and approximately 1.5 cm^3 for the LCLS.

For estimating the total deposited energy vs. time, the charge and energy carried by the linac bunch structure in both the Madey and LCLS cases are shown in Fig. 4. We note that, per second, each of the ten macropulses from the Madey linac carries ~ 250 J, while each of the 120 single-pulse macropulses from the SLAC linac carries ~ 12 J.

4. Numerical Results

Prior theoretical and experimental studies of quenching threshold levels in potted SC coil structures have provided strong evidence that the critical quantity is deposited energy density, and numerical values on the order of 100μJ/cm^3 (e.g., approximately 150μJ/cm^3 for SC wire consisting of 180 NbTi filaments [11]) have been measured for this parameter [12]. Using this value as a convenient referent, and assuming a potted LCLS structure, we first calculated the total amount of energy required to quench an annular ring in both the Madey and LCLS cases and then expressed this as a fraction of the total energy in each macropulse. For the Madey case this "critical quenching fraction" was calculated to be $2.3\text{x}10^{-6}$, and $1.9\text{x}10^{-5}$ for the LCLS case. In Figure 5 we show the results of selected sets of EGS4 runs for both structures.

In both graphs the energy deposited in the annular SC regions is shown as a fraction of the total electron energy vs. distance down the undulator axis. For the left-hand graph the scatterer was Madey's 254 μ Mo foil, which intercepted the full beam. In the right-hand graph the scatterer is a 20-cm W collimator with a 50 μ aperture, which passes approximately 90% of the beam The upper quenching threshold drawn on the right-hand side is valid for this assumption, viz., for a scattered macropulse energy of 1.2 J.

A number of preliminary studies on a number of solid W foils of different thicknesses were performed before the results in the right hand graph were arrived at. Initially, the assumed outside radius (collim_OR in Fig. 3) was set to 5mm. With this dimension the effect of increasing the W thickness on the deposited energy was found to be weak. Further runs showed that this was caused by substantial energy showering out through the sides of the foil and into the SC material. Increasing the outside W foil radius to 5 cm eliminated this effect and the deposited energy vs. foil thickness was found to show the proper exponential dependence (see "no hole" curve in Fig. 6). Next, a 50 μ hole was introduced, a Gaussian distribution of particle angles with a 10 μ-rad standard deviation was assumed, and the dependence of deposited energy vs. W collimator thickness was studied. The results are represented by the curve labeled "50 micron hole" in Fig. 6. Even though only 10% of the beam is being scraped, the results clearly demonstrate that electromagnetic showers escaping into the aperture and propagating down the axis can contribute significantly to the total amount of energy scattered through the collimator.

5. Discussion

For the Madey experiment, the EGS4 results graphed on the left in Fig. 5 appear to suggest that conditions for quenching were exceeded by almost three orders of magnitude. In the actual experiment, however, the quenching would reportedly stop when the linac current was reduced by factors of 10-100 [5]. This discrepancy can be accounted for by: 1) our lack of precise knowledge of the critical quenching density for the actual Madey structure, 2) the lack of precisely recorded linac running parameters during the quenching episodes, and 3) our assumption that the full amount of energy in a macropulse actually accumulated in the SC material before being conducted away. In the first case, we note that both theoretical [12,13] and experimental [14] studies have indicated that the actual critical quenching density is dependent on the rate at which heat can be transported out of the SC coils; viz., on the materials, design, and engineering details of the structure. For example, according to Allinger et al [14] the immersion of SC coils directly in He, along with the use of high-conductivity Al in construction, inhibited the spread of normal zones even under direct deposition on the order of 100 J into the SC coil with a multi-GeV proton beam. The associated figures suggest that the actual critical quenching density may have been raised by 1-2 orders of magnitude over our cited 150 $\mu J/cm^3$ figure. Second, the linac current and time structure parameters cited for the Madey quench study (Fig. 2, top) should not be considered reliable to within factors of 2-3. Next, since the Madey macropulse was approximately 5 ms long, the actual heat removal rate in his structure may have prevented the accumulation of the full amount of macropulse energy (250 J) inside the SC volume, and estimates of this effect have not been included in the present study. Finally, as discussed above, the model we employed did not include the magnetic field. To within all these qualifications, however, the EGS4 results can be interpreted as generally corroborating the quenching observed by Madey.

Apart from these issues, additional factors are relevant in interpreting the LCLS results. Although the deposited energy is a factor of 20 smaller than the upper critical threshold (Fig. 5, right), this is for a beam scraping factor of 10%. In actual running, beam jitter (angular and positional) could presumably cause the fraction of scattered beam to occasionally approach 100%, as well as elevate the fraction of energy deposited into the SC coils. This could easily raise the deposited energy level above the lower threshold. At the same time, it should be noted that in an actual collimator design the hole geometry can be optimized to inhibit the escape of E&M shower energy to levels well below those operative in the present case [15]. Furthermore, the collimator could, in principle, be removed significantly further upstream or even installed in an off-axis chicane. Given all these considerations, a major conclusion of our study is that the design and engineering details of both the collimator and an SC undulator structure (in particular, potted vs. non-potted construction, cooling scheme, etc.) are likely to be critical, and that it will be advisable to employ EGS4 in the design process. In future r&d we plan to analyze more realistic EGS4 models of the bifilar helical undulator, including the magnetic field; develop optimized collimator designs; and perform actual quenching experiments on small models or engineering prototypes in which EGS4 will be used in a simulatory role. Further analytical and EGS4 studies of the LCLS system are also being planned to investigate the effects E&M showers induced by gas within the collimator aperture and in the long bore of the undulator.

6. Acknowledgments

In undertaking and interpreting the research presented here, interactions and discussions with Shlomo Caspi, Lawrence Dresner, David Larbalestier, Ron Scanlan, Todd Smith, Steve St. Lorant, Clyde Taylor, and many members of the LCLS research group were invaluable. We thank John Madey for permission to use Fig. 2. Our work was supported in part by the Department of Energy Offices of Basic Energy Sciences and High Energy and Nuclear Physics and Department of Energy Contract DE-AC03-76SF0015.

7. References

[1] R. Tatchyn, K. Bane, R. Boyce, G. Loew, R. Miller, H.-D. Nuhn, D. Palmer, J. Paterson, T. Raubenheimer, J. Seeman, H. Winick, D. Yeremian, C. Pellegrini, J. Rosenzweig, G. Travish, D. Prosnitz, E. T. Scharlemann, S. Caspi, W. Fawley, K. Halbach, K.-J. Kim R. Schlueter, M. Xie, R. Bonifacio, L. De Salvo, P. Pierini, "Prospects for High Power Linac Coherent Light Source (LCLS) Development in the 1000Å-1Å Wavelength Range." AIP Conference Proceedings 332, D. C. Eder and D. L. Matthews, eds., 320(1994).

[2] S. Caspi, R. Schlueter, R. Tatchyn, "High-Field Strong-Focusing Undulator Designs for X-Ray Linac Coherent Light Source (LCLS) Applications," presented at the IEEE PAC95, Dallas, TX, May 1-5, 1995, ms. FAQ-23, SLAC-PUB-95-6885.

[3] M. Xie, "Design Optimization for an X-Ray Free Electron Laser Driven By SLAC Linac," presented at the IEEE PAC95, Dallas, TX, May 1-5, 1995, ms. TPG-10.

[4] L.R. Elias, and J. M. Madey, "Superconducting helically wound magnet for the free-electron laser," Rev. Sci. Instrum. 50(11), 1335(1979).

[5] Todd Smith, private communication.

[6] Lawrence Dresner, Ron Scanlan, Shlomo Caspi, Todd Smith, private communication.

[7] K. L. Bane, T. O. Raubenheimer, J. T. Seeman, "Electron Transport of a Linac Coherent Light Source," Proc 1993 Particle Accelerator Conference, IEEE Catalog No. 93CH3279-7, 596(1993).

[8] W. R. Nelson, H. Hirayama, and W. O. Rogers, "The EGS4 Code System," SLAC-Report-265, December 1985.

[9] W. R. Nelson, et al, "The EGS Code - A Spinoff to Medicine," in Proceedings of a Workshop on Applications of Accelerators, SLAC, December 1-2, 1993, W. B. Hermannsfeldt, A. M. Sessler, and J. R. Alonso, eds., SLAC-430, pp. 24 ff.

[10]W. R. Nelson, "Properties of the EM Cascade, a Tutorial Utilizing High Resolution Color Graphics," SLAC-PUB-4203, February, 1987.

[11]D. J. Waltman, M. J. Superczynski, F. E. McDonald, "Energy Pulses Required to Quench Potted Superconducting Magnets at Constant Field," IEEE Trans. Mag. 17(1), 1056(1981).

[12]L. Dresner, Stability of Superconductors, Selected Topics in Superconductivity, S. Wolf, ed., Plenum Press, New York, 1995, Chapter 4.

[13]E. W. Collings, Applied Superconductivity, Metallurgy, and Physics of Titanium Alloys (Volume 2, Applications), The International Cryogenics Monograph Series, K. D. Timmerhaus, A. F. Clark, eds., Plenum Press, New York, 1986, Sections 24.5 ff, 25.

[14]J. Allinger, G. Danby, H. Foelsche, J. Jackson, D. Lowenstein, A. Prodell, W. Weng, "Quench Thresholds in Operational Superconducting Magnets," IEEE Trans. Mag. 15(1), 119(1979).

[15]S. Mao, J. Liu, W. R. Nelson, "Using the EGS4 Computer Code to Determine Radiation Sources Along Beam Lines at Electron Accelerators," ANS Topical Meeting on New Horizons in Radiation Protection and Shielding, Pasco, WA, April 26-May 1, 1992, SLAC-PUB-5723.

SLAC-PUB-95-6970
August 1995

Figure Captions

Figure 1. Schematized helical bifilar geometry (1a) and a cylindrically-symmetrized equivalent geometry (1b) utilized in simulating scattered-energy deposition with the EGS4 particle-tracking code.

Figure 2. Cross sectional view of Madey's SC helical bifilar undulator structure. (a) outer Al shield; (b) epoxy; (c) SC solenoidal winding; (d) bifilar helical SC winding; (e) Delrin mandrel; (f) Cu vacuum duct.

Figure 3. Side view of the general symmetrized geometry of the Madey and LCLS undulators, including the cryostat and upstream scattering elements. The dimensions and materials associated with each undulator case are listed in the table. The volumes into which the entire structure is partitioned are all axi-symmetric annular rings.

Figure 4. Linac pulse structures of the Madey (top) and LCLS (bottom) experiments. Bunch charge is plotted as a function of time, allowing the peak and average current/bunch and energy/bunch to be estimated.

Figure 5. EGS4 simulations of the fractional energy deposited into the SC material for the Madey (left) and LCLS (right) structures. The LCLS study assumes a Gaussian distribution of electron angles with a standard deviation of 10 μ-radians. The estimated quenching threshold levels corresponding to the assumed fraction of beam intercepted by the screens are indicated by the dotted lines. Selected dimensions of the screens are listed in each graph.

Figure 6. Graph showing the effect of the LCLS W screen thickness on the energy fraction deposited into the undulator's SC regions, with vs. without a 50 μ collimating aperture.

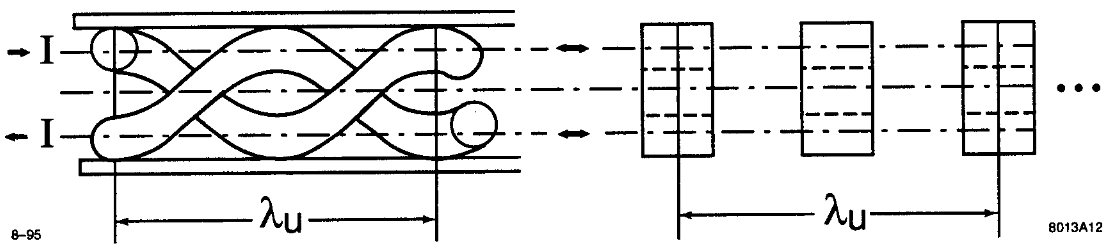

Fig. 1

SLAC-PUB-95-6970
August 1995

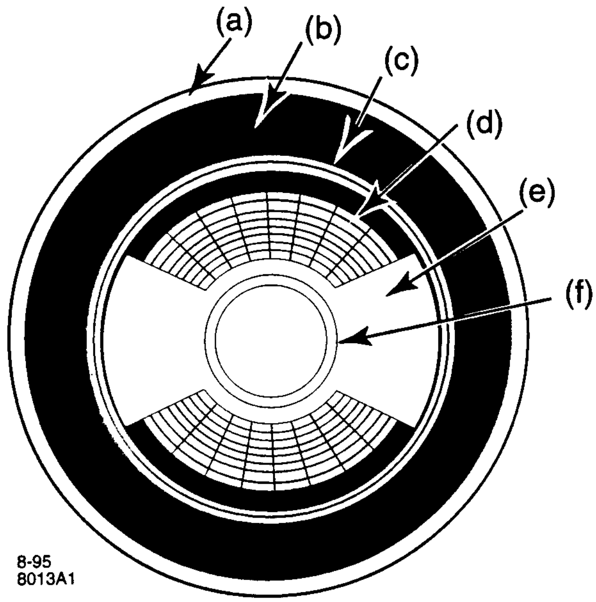

Fig. 2

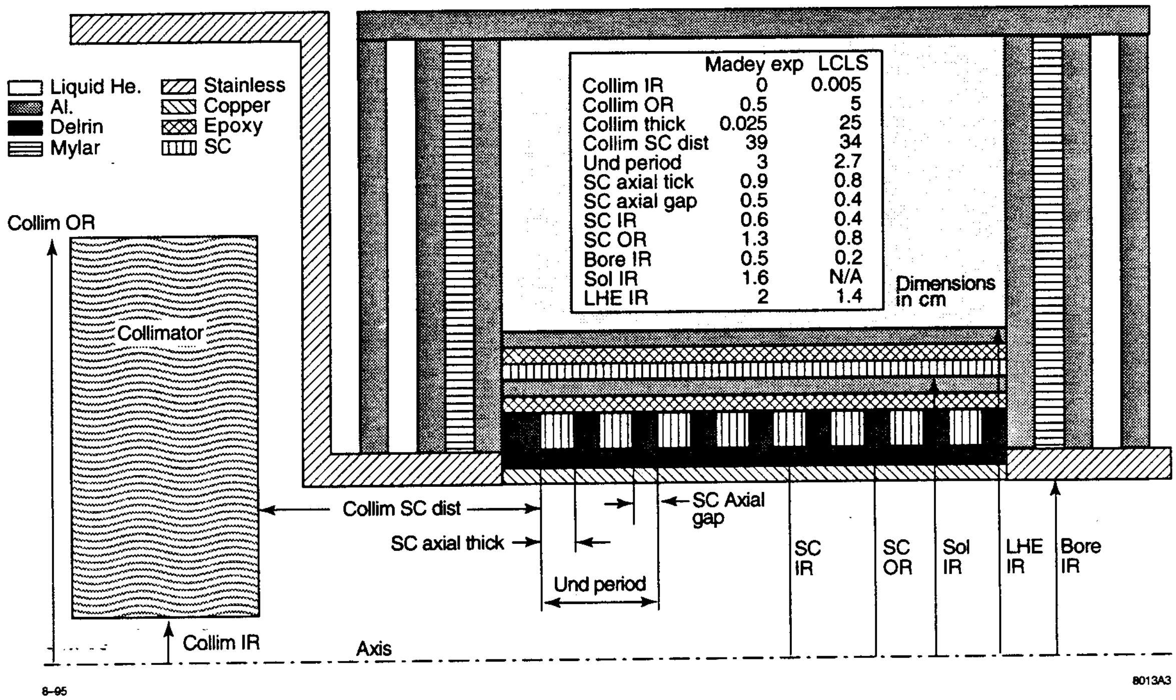
Liquid He.
Al.
Delrin
Mylar
Stainless
Copper
Epoxy
SC
Collim OR
Collimator
Collim IR
Madey exp LCLS
Collim IR 0 0.005
Collim OR 0.5 5
Collim thick 0.025 25
Collim SC dist 39 34
Und period 3 2.7
SC axial tick 0.9 0.8
SC axial gap 0.5 0.4
SC IR 0.6 0.4
SC OR 1.3 0.8
Bore IR 0.5 0.2
Sol IR 1.6 N/A
LHE IR 2 1.4
Dimensions in cm
Collim SC dist
SC axial thick
SC Axial gap
Und period
SC IR
SC OR
Sol IR
LHE IR
Bore IR
Axis
8-95
8013A3

Fig. 3

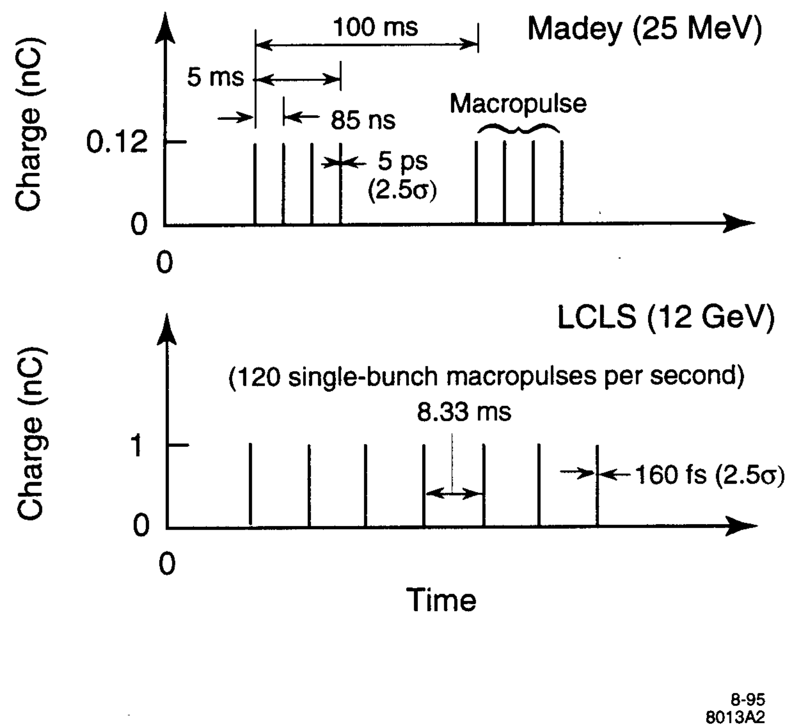
100 ms
Madey (25 MeV)
5 ms
85 ns
Macropulse
0.12
5 ps
(2.5σ)
Charge (nC)
0
0
LCLS (12 GeV)
(120 single-bunch macropulses per second)
8.33 ms
1
160 fs (2.5σ)
Charge (nC)
0
0
Time
8-95
8013A2

Fig. 4

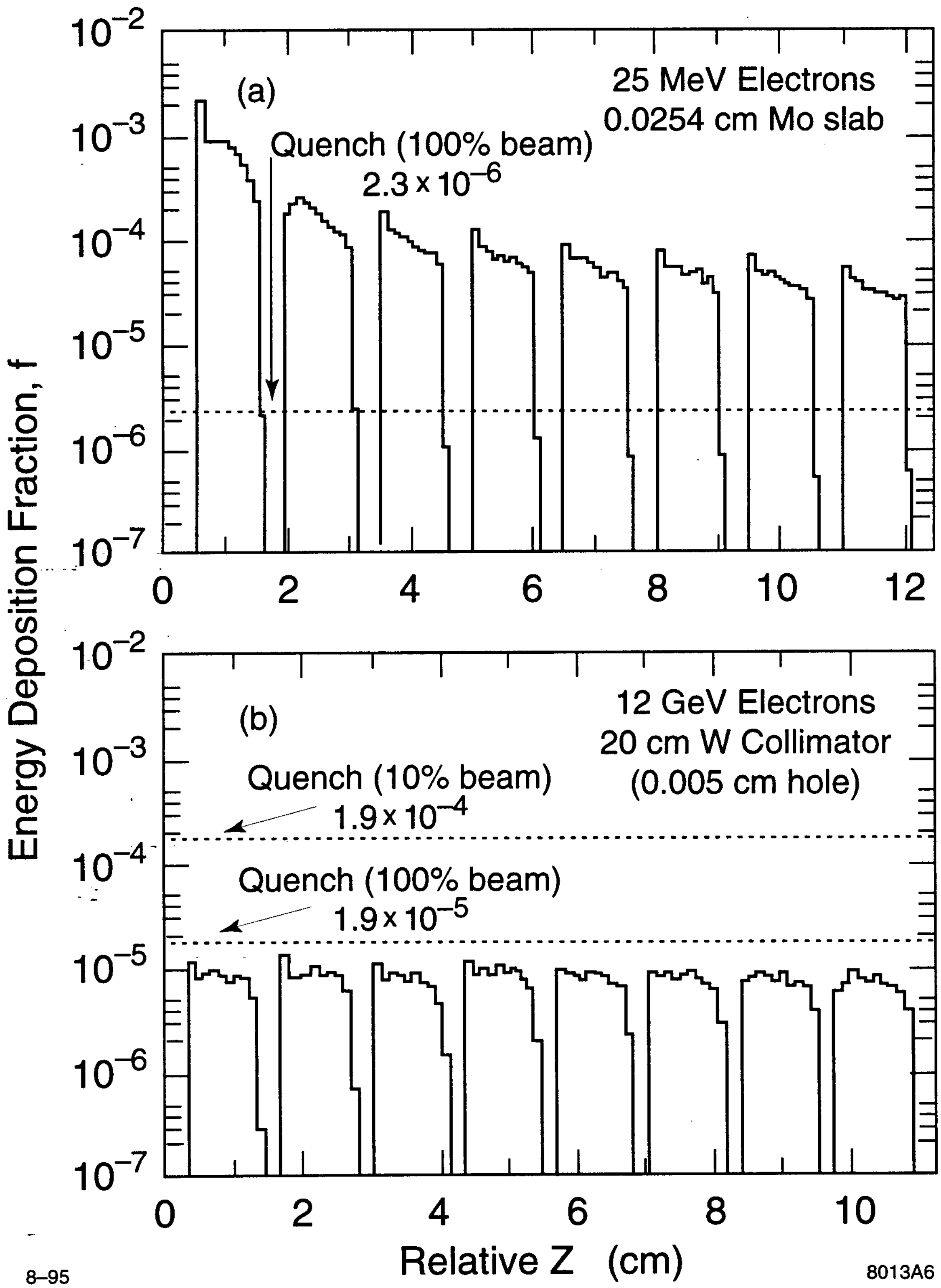
(a)
25 MeV Electrons
0.0254 cm Mo slab
Quench (100% beam)
2.3×10^{-6}
(b)
12 GeV Electrons
20 cm W Collimator
(0.005 cm hole)
Quench (10% beam)
1.9×10^{-4}
Quench (100% beam)
1.9×10^{-5}
Energy Deposition Fraction, f
Relative Z (cm)
8–95
8013A6

Fig. 5

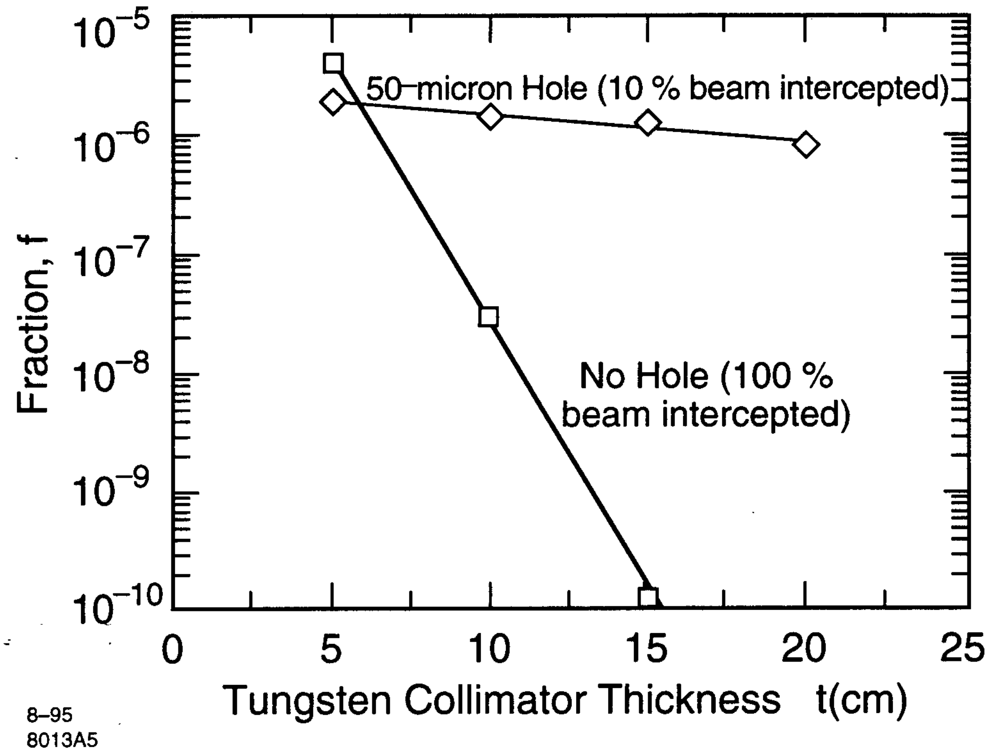
10^-5
10^-6
10^-7
10^-8
10^-9
10^-10
Fraction, f
50-micron Hole (10 % beam intercepted)
No Hole (100 % beam intercepted)
0
5
10
15
20
25
Tungsten Collimator Thickness t(cm)
8–95
8013A5

Fig. 6